

# DIPOLE ARRAY EXCITED BY SLOTS IN ITS COAXIAL FEEDER

Dušan ČERNOHORSKÝ, Zdeněk NOVÁČEK  
Dept. of Radio Electronics  
Brno University of Technology  
Purkyňova 118, 612 00 Brno  
Czech Republic

## Abstract

*Technical analysis of the coaxial dipole-array excited by periodically distributed slots in common coaxial feeder is presented. The lossy transmission-line theory is applied for determination of the current on all parts of the system. Calculated results support some properties of the system, especially radiation pattern and the input impedance.*

## Keywords

Dipole array, slot excited dipole, feeding of dipole arrays, two-point excited radiators

## 1. Introduction

Some communication systems require vertically polarized antennas which are omnidirectional in the horizontal plane and which present certain significant directivity in elevation (in the vertical plane). Such antennas can be realized like vertically situated linear arrays of vertical dipoles. But the design of a sufficiently simple feeding system together with a suitable and mechanically compact construction brings troubles in practice.

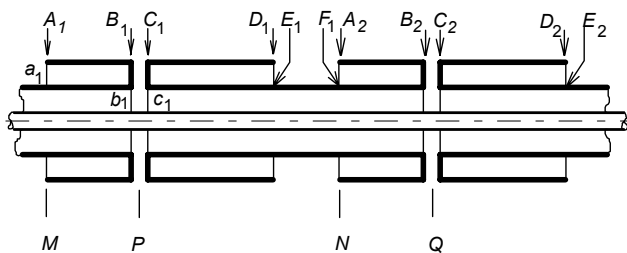


Fig. 1 The lengthwise cross-section of the analysed array (schematic sketch). The system is vertically situated in practice.

An interesting solution of this problem occurs sporadically in practice. The common vertical coaxial feeder has periodically distributed narrow slots in its sheath (outer conductor, see Fig.1). Relatively short tubes ("sleeves") are put on the cable and connected with opposite sides of each

slot. The outer surfaces of these tubes act like dipole arms of the array. The inner part of each tube is a coaxial resonator whose reactance connects ends of dipole arms with the outer surface of the main feeder. In case that the resonators are exactly tuned to the operating frequency, the arm ends are insulated and the whole system operates like a linear dipole array. In the opposite case, the resonators reactances are finite and the outer surface of the main feeder grows into an active (radiating) part of the antenna.

Note that the idea of excitation of linear radiators by slots is applied (in modified form) also at the "ARPO" antenna [2]. Here, we shall be engaged exclusively in the system described above and drawn in Fig. 1.

Some properties of one section alone (e.g. from  $A_1$  to  $F_1$  in Fig.1) of the described antenna are investigated in [1]. The analysis is based on the lossy transmission-line theory and is limited by several suppositions:

- The length of one dipole arm is exactly  $\lambda/4$  and the corresponding resonator inside is also exactly tuned to the operating frequency.
- The electrical length of the section ( $A_1-F_2$ ) is the same like the electrical length of the main feeder between corresponding points.
- These electrical lengths are exactly equal to  $2\pi$ .

The results of the analysis shows that one section alone can behave either like two-element dipole array with opposite phase in elements or nearly like one dipole. The behaviour depends on the prolongation of one dipole arm and on the reactance of the detuned resonator.

In the paper, a more general solution is shown. The limitations mentioned above need not be met. The length of the main feeder between  $P$ ,  $Q$  as well as the length of its radiating surface may be arbitrary (and they need not be equal), both resonators (cavities) may be detuned and the number of sections is not limited. But in the same way as in [1], lossy transmission-line theory is applied and the electromagnetic coupling between sections is neglected. This last assumption may be well accepted since the radiating part of the antenna is treated as a transmission-line. Effect of mutual coupling between its sections is largely included in the value of common characteristic impedance (calculated for line as the whole, not for each section separately).

## 2. Coaxial Dipole Array -Equivalent Set of Transmission-Lines

The complete antenna system has three parts. The bottom part (input part inclusive the feeder), the central (radia-

ting) part and the top (terminating) part. The bottom and the top parts are discussed later. The central part consists of several identical sections (e.g.  $P-Q$  in Figs. 1 or 2). In our analysis, each of these sections will be treated as a pair of separate transmission lines, whose inputs as well as outputs are connected in series. One of these transmission lines is the mean coaxial line (between the cross-sections  $P$  and  $Q$  in Fig. 1 or Fig. 2). The second transmission line is the outer surface of the system, which radiates. This (second) line has three parts ( $C_1-D_1, E_1-F_1, A_2-B_2$ ) on each section. These parts are connected via reactances of detuned resonators (cavities). "Back conductor" of this outer transmission line is the ground or imaginary conducting surface in infinity.

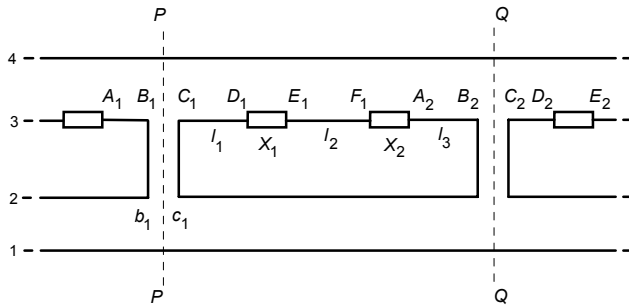


**Fig. 2** Equivalent scheme of the antenna system. 1+2: the coaxial line. (the wire 2 is the internal surface of the sheath); 3: the outer surface of the coaxial with resonators reactances; 4: remote conducting surface (ground)

In agreement with just described idea, the equivalent scheme in Fig. 2 can be drawn. Both transmission lines (inner one - the coaxial, and the outer one - the radiating surface) are drawn as two-wire lines. The wire 1 is the inner conductor of the coaxial, the wire 2 is the inner surface of the coaxial sheath. The wire 3 is the outer (radiating) surface of the main line and the wire 4 is the "ground" in infinity. Notation of individual points graphically corresponds to Fig. 1. The relative independence of both transmission lines is accented by a greater separation between them. Actually, the "wires" between points  $b_1-B_1, c_1-C_1$  etc., connecting the inner and the outer surfaces of the coaxial sheath, are very short (they are opposite fronts of slots on sheath). Therefore, the current at  $B_1$  is equal to that in  $b_1$ , etc.

### 3. Voltages and Currents in the System

#### 3.1 The central part

Between the output voltage and current and the voltage and current at any point  $O$  of a homogeneous transmission-line, the following well-known relations are valid:

$$\begin{aligned} U_{in} &= U_{out} \cdot \cosh(\gamma z) + I_{out} \cdot Z_0 \cdot \sin(\gamma z) \\ I_{in} &= U_{out} / Z_0 \cdot \sinh(\gamma z) + I_{out} \cdot \cosh(\gamma z) \end{aligned} \quad (1)$$

$Z_0$  is the characteristic impedance of the line,  $\gamma = \beta + j\alpha$  is the propagation constant and  $z$  is the distance from the line output to the point  $O$ .  $U$  and  $I$  are the complex amplitudes

of total voltage and current. Substituting total line-length  $l$  instead of the variable  $z$ , we obtain relations between output- and input quantities  $U_{out}, I_{out}, U_{in}, I_{in}$ . In matrix form, these relations are:

$$\begin{bmatrix} U_{in} \\ I_{in} \end{bmatrix} = \begin{bmatrix} \cosh(\gamma l) & Z_0 \cdot \sinh(\gamma l) \\ \sinh(\gamma l) / Z_0 & \cosh(\gamma l) \end{bmatrix} \begin{bmatrix} U_{out} \\ I_{out} \end{bmatrix} = [A] \begin{bmatrix} U_{out} \\ I_{out} \end{bmatrix} \quad (2)$$

The matrix  $[A]$  keeps similar properties like the transmitting matrix: e.g. the resulting matrix of a cascade connection of several elements is equal to the product of  $A$ -matrices of the elements alone.

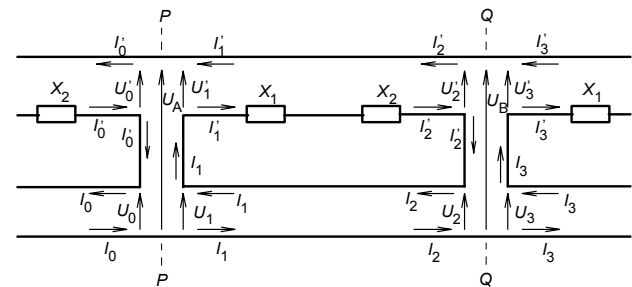


**Fig. 3** Equivalent scheme as in Fig. 2. The voltages and currents are denoted here

The section  $P-Q$  of the coaxial transmission line is a homogeneous section and (1) can be applied directly. According to the notation in Fig. 3, output quantities can be denoted by subscript 2, and input quantities by subscript 1. We rewrite the equations (1) to the form

$$\begin{aligned} U_1 &= aU_2 + bI_2 \\ I_1 &= cU_2 + dI_2 \end{aligned} \quad (3)$$

where

$$\begin{aligned} a &= \cosh(\gamma l) & c &= Z_0 \sinh(\gamma l) \\ b &= \sinh(\gamma l) / Z_0 & d &= \cosh(\gamma l) \end{aligned} \quad (4)$$

and  $l_c, \gamma_c$  and  $Z_{0c}$  are the parameters of the coaxial line.

The outer transmission line (wires 3 and 4) consists of five elements in cascade. They are three transmission-lines ( $C_1-D_1, E_1-F_1, A_2-B_2$ ) and two reactances  $X_1, X_2$ . Its  $A$ -matrix is

$$[A'] = [A_1][A_{x1}][A_2][A_{x2}][A_3] = \begin{bmatrix} a' & b' \\ c' & d' \end{bmatrix} \quad (5)$$

$[A_1], [A_2]$  and  $[A_3]$  are  $A$ -matrices of the type (1) of individual parts of the outer surface ( $C_1-D_1, E_1-F_1, A_2-B_2$ ) and

$$[A_{x1,2}] = \begin{bmatrix} 1 & jX_{1,2} \\ 0 & 1 \end{bmatrix} \quad (6)$$

are the matrices of series reactances  $X_{1,2}$ .

The equations analogous with (3) which are valid for the outer transmission line (wires 3, 4) are:

$$\begin{aligned} U_1' &= a'U_2' + b'I_2' \\ I_1' &= c'U_2' + d'I_2' \end{aligned} \quad (7)$$

The matrix elements  $a'$ ,  $b'$ ,  $c'$ ,  $d'$  must be evaluated from (5). (All quantities relevant to outer (radiating) transmission-line are differentiated by dashes in the whole text).

Besides relations (3) and (7), some other relations more follow from the scheme in Fig. 3. They are:

$$\begin{aligned} I_0 &= I_1 & I_0' &= I_1' & U_1 + U_1' &= U_A & (8a, b, c) \\ I_2 &= I_3 & I_2' &= I_3' & U_2 + U_2' &= U_B & (8d, e, f) \end{aligned}$$

The most important for our consideration are the equalities

$$I_1' = I_1 \quad I_2' = I_2 \quad (9)$$

that follows as the consequence of negligible distance between the inner- and outer- surfaces of the coaxial sheath.

The deduced relations enable the numerical analysis of the current distribution on the central part of the system. Let us suppose for this moment that the analysis proceeds (as very often in similar situations) from the end to source. Suppose later that, for instance, the voltages  $U_3$  and  $U_3'$  and the currents  $I_3 = I_3'$  in Fig. 3 are known. The section P-Q is now the subject of our investigation. Its output currents are known immediately:  $I_2 = I_2' = I_3 = I_3'$  (see eqs. 8d, e). For determination of  $U_2$  and  $U_2'$ , the condition (9b) must applied. The voltage  $U_b$  will be decomposed to the voltages  $U_2$  and  $U_2'$  in such manner that currents  $I_1$ ,  $I_1'$  (at the cross-section P) are identical (see eqn. 9). When  $I_1 = I_1'$ , then also the right sides of (3b) and (7b) must be equal and from this equality, the following formulae can be found:

$$\begin{aligned} U_2 &= \frac{c'}{c+c'}U_B + \frac{d'-d}{c+c'}I_2 \\ U_2' &= \frac{c}{c+c'}U_B - \frac{d'-d}{c+c'}I_2 \end{aligned} \quad (10)$$

Now, voltages and currents at the ends of both lines (the outer- and the inner-one) on the section P-Q are known. The input voltages and currents ( $U_1$ ,  $U_1'$ ,  $I_1$ ,  $I_1'$ ) can be obtained using eqns. (3) and (7). Finally,  $U_A = U_1 + U_1'$ .

The situation at the cross-section P is now identical with that, which was considered at cross-section Q several lines above. That means, the voltage  $U_A$  must be decomposed in  $U_0$  and  $U_0'$  using equations (10), etc. In this way, section by section, we can proceed up to array input.

### 3.2 The Top and Bottom Parts

The equations analogous to (3) and (7) together with equalities (8) enable to find voltages and currents in the

remaining parts of the system. We shall start with the antenna top.

The central part, discussed in previous subsection, has two "output terminals": the coaxial line and the outer surface of the sheath. The coaxial line may continue still certain length and then, it is terminated by a load  $Z_L$ . The load can be of various kinds. It can be the short circuit, real or complex impedance or (in special cases) also another antenna. Any case, value of load impedance must be known.

For the explanation of the situation on the outer surface of the coaxial sheath, let us suppose that the section P-Q in Fig. 1 is the last one and the antenna top part is the part from the cross-section Q to the right. The outer (radiating) surface has (at least) three elements: The dipole arm  $C_2-D_2$ , the resonator reactance between  $D_2-E_2$  and the remaining part of the surface up to the coaxial-line end.

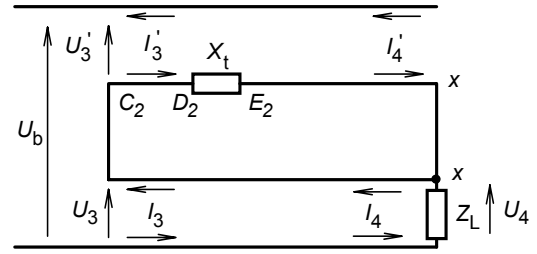


Fig. 4 The equivalent scheme of the antenna top part.

In agreement with the previous treatments, the equivalent scheme in Fig. 4 can be applied for the antenna top part. One supposes that the coaxial load  $Z_L$  is "hidden" inside and no others conducting objects are connected to the coaxial line end. As the currents  $I_4$  forwards and backwards in the coaxial line interior must be equal, no current flows through the connection  $x-x$  (Fig. 4). The outer conductor is open-ended and

$$I_4' = 0 \quad (11)$$

When the dimensions of individual elements in the scheme (Fig. 4) are known, the matrices of the inner- and outer transmission-line can be found the same way as in 3.1:

$$[A_t] = \begin{bmatrix} a_t & b_t \\ c_t & d_t \end{bmatrix} \quad [A'_t] = \begin{bmatrix} a'_t & b'_t \\ c'_t & d'_t \end{bmatrix}$$

Consequently

$$U_3 = a_t U_4 + b_t I_4 \quad I_3 = c_t U_4 + d_t I_4 \quad (12)$$

$$U_3' = a'_t U_4 + b'_t I_4 \quad I_3' = c'_t U_4 + d'_t I_4 \quad (13)$$

Substituting  $I_4' = 0$  and  $U_4 = Z_L I_4$ , all the others voltages and currents can be expressed as functions of the load current  $I_4$

$$U_4' = (c Z_L + d)/c'_t I_4$$

$$U_3' = a'_t U_4$$

$$(14a, b, c, d)$$

$$U_3 = (aZ_L + b)I_4$$

$$I_3 = I'_3 = cU'_4$$

The equations (14b, c, d) give the quantities that are needed for the analysis of the central part.

Now, we shall suppose that the element  $P-Q$  in Fig. 1 is the first one and all from the cross-section  $P$  to the left is the antenna bottom. The coaxial line leads to the left up to the source (transmitter). It is perfectly screened so that no high-frequency connection between outer- and inner sheath surfaces exists. The outer (radiating) surface consists of the arm  $A_1-B_1$ , the reactance  $X_b$  between  $A_1$  and  $a_1$  and of certain length  $l_{b2}$  up to the source, where it is earthed. The equivalent scheme is drawn in Fig. 5.

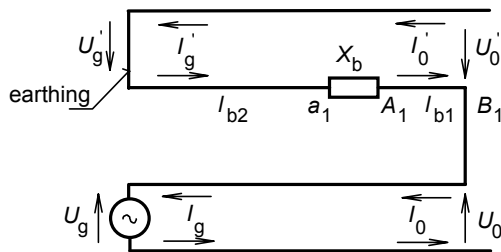


**Fig. 5** The equivalent scheme of the bottom part. The outer transmission-line is fed on the right side and acts like a load. The voltage  $U_o'$  has reversed direction

The coaxial-line matrix  $[A_b]$  can be found in the same way as above. But in contradistinction to previous situations, the outer transmission-line is fed on its right side ( $U'_0$ ) and is short-circuited at its end (left). Therefore the matrix  $[A'_b]$  must be assembled from the right (input) to the left (end):

$$[A'_b] = [A_{l_{b1}}] [A_{X_b}] [A_{l_{b2}}] = \begin{bmatrix} a'_b & b'_b \\ c'_b & d'_b \end{bmatrix} \quad (15)$$

The equations valid for the antenna bottom are:

$$U_g = a_b U_0 + b_b I_0 \quad I_g = c_b U_0 + d_b I_0 \quad (16)$$

$$U'_g = a'_b U'_0 + b'_b I'_0 \quad I'_g = c'_b U'_0 + d'_b I'_0 \quad (17)$$

Due to the outer-surface earthing,  $U_g' = 0$  and the equation (17) simplifies. It is easy to find the following relations:

$$U'_0 = -I'_0 b'_b / a'_b \quad U_0 = U_A + U'_0 \quad (18)$$

The voltage and current at the feeding point (generator) are given by (16). The impedance at the feeding point is

$$Z_{in} = U_g / I_g \quad (19)$$

and the current flowing into the earth

$$I'_g = I'_0 / d'_b \quad (20)$$

The values of  $I'_0$  and  $U_A$  follows from the antenna central part analysis.

## 4. The Calculation Procedure

One supposes that all antenna dimensions, resonator reactances and the load impedance  $Z_L$  are known. Using suitable formula, the characteristic impedances of individual transmission-lines can be calculated. The own calculation procedure starts by an arbitrary choice of the load current  $I_4$  and by the choice of attenuation constant (acceptable value is about  $\beta\lambda = 1$ ). According to the structure of individual elements, their  $A$ -matrices are calculated.

Then the output- and input voltages and currents of individual parts of the system will be found. Eqns. (14) are valid for the antenna top part. For the central part, eqns. (10), (3) and (7) will be applied repeatedly. Eqn. (18) together with (8a,b) and (9) give the results for the bottom part. Finally, the complex input impedance of the whole antenna follows from equations (16) and (19). That is the resulting input impedance according to transmission-line theory.

In the case that the impedance at some slot (observed inside the coaxial feeder) is required, we handle the scheme in Fig. 3. It holds for the  $n$ -th slot:

$$Z_{slot} = (U_{n+1} - U_n) / I_n$$

The values of  $U_{n+1}$ ,  $U_n$  and  $I_n$  are known from the previous central part analysis.

The current distribution on individual transmission-lines is calculated by means of (1). The reactances may be passed using the matrices (6). Knowing the current distribution, the calculation of radiation pattern is a classical task. Finally, the value of attenuation constant beta can be made more accurate in the same way like in [1]: the real part of input impedance calculated according to transmission-line theory (19) should be nearly equal to that calculated from radiated power (radiation pattern).

## 5. Calculated Results

The relations deduced above were applied to several dimensional variations of the coaxial dipole array. All the presented results have to do with an array, which has two sections (three slots) and quarter-wave long bottom- and top parts. Return us once more to Fig. 1 for precise description of the calculated antenna. The part from  $M$  to  $Q$  represents the lower half of the antenna, from  $Q$  to the right follow one section of type  $PQ$  and the antenna top, symmetrical with  $MP$ . The coaxial line is short-circuited at its end. In all presented examples, the coaxial-line characteristic impedance is equal to  $50 \Omega$  and the antenna-radiating surface has common characteristic impedance  $200 \Omega$ .

The array dimensions are described by lengths  $l_1 = C_1 D_1$ ,  $l_2 = E_1 F_1$  and  $l_3 = A_2 B_2$  of one section (Fig. 1). To remove the frequency dependence of all results, dimensions are not presented in meters, but in electrical lengths  $\alpha l_i = 360 l_i/\lambda$  [grad]. Also coaxial-line length  $l_k$  between

two neighbouring slots is presented as  $\alpha_g l_k = 360 l_k / \lambda_g$  (the subscript  $g$  denotes quantities of the coaxial-line). The values of reactances  $X_1$  and  $X_2$  make the description of each array complete.

In following figures, computed current distribution and radiation pattern in vertical plane for various antenna dimensions are presented. The direction  $\theta = 0^\circ$  is the horizontal one and  $\theta = 90^\circ$  is the vertical direction up. The antenna dimensions as well as the input impedance and the directivity factor  $D_{max}$  are written in the Figure text. Also the value of attenuation constant  $\beta \lambda$  can be of interest for some readers.

In the first set of examples, the antenna is considered as an equiphasic-array of three "conventional" dipoles. Thus, the starting dimensions are:  $\alpha l_1 = \alpha l_3 = 90^\circ$ ,  $\alpha_g l_k = 360^\circ$  and the reactances  $X_1 = X_2$  are very great. These starting dimensions are successively modified.

The results for a trio of "classical" half-wave dipoles ( $\alpha l_1 = \alpha l_3 = 90^\circ$ ,  $\alpha_g l_k = 360^\circ$ ,  $X_1 = X_2 \rightarrow \infty$ ) are shown in Fig. 6. This array has a "nice" main lobe in horizontal direction. The side-lobe level is about -10 dB, the main lobe width (in -3 dB level) is about  $2.9^\circ = 18^\circ$  and the directivity factor  $D_{max} = 5.3$  dB. The input impedance is about  $(205 + j 28) \Omega$  and that is nearly a treble of single dipole value. The prolongation of dipole arms up to 135 grad does not affect (practically) the radiation pattern, but the input impedance increases up to  $700 \Omega$ .

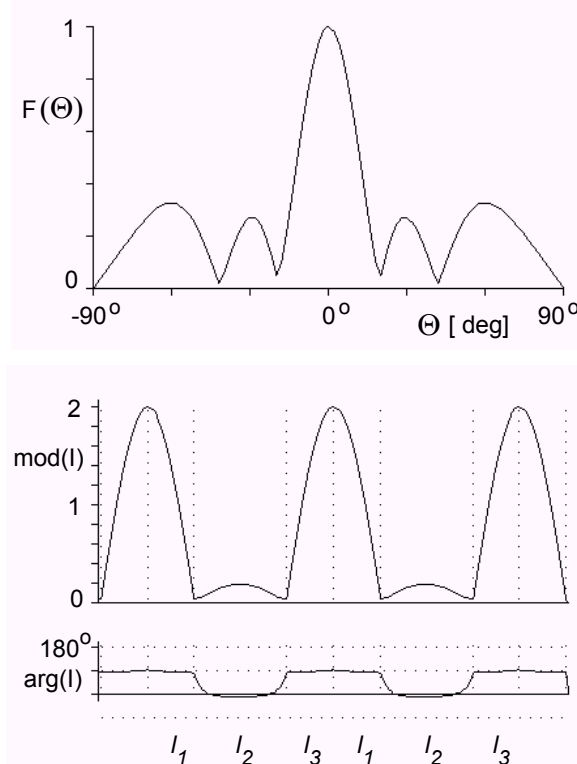


**Fig. 6** Radiation pattern and current distribution of coaxial array.  
 $\alpha l_1 = 90^\circ$ ,  $\alpha l_2 = 180^\circ$ ,  $\alpha l_3 = 90^\circ$ ,  $X_1 = X_2 = -10\ 000 \Omega$ ,  
 $\alpha_g l_k = 360^\circ$ .  $D_{max} = 5.3$ ,  $Z_{in} = (205 + j 28) \Omega$ ,  $\beta \lambda = 0.82$

When the dipoles dimensions remain the same as in Fig. 6, but the coaxial feeder is "detuned" (that means  $\alpha_g l_k \neq 360^\circ$ ), a shift of the main lobe direction appears (Fig. 7) and the input impedance drops. The radiation pattern on a whole is slightly deformed. Due to this fact, the feeder detuning (and consequently main lobe shift) must not be too great. Maximum lobe deflection is about  $10^\circ$ .

When the feeder electrical length  $\alpha_g l_k > 360^\circ$ , the main lobe direction is shifted to greater values of elevation angle  $\Theta$ . On the contrary, when  $\alpha_g l_k < 360^\circ$ , the main lobe is tilted to the earth.

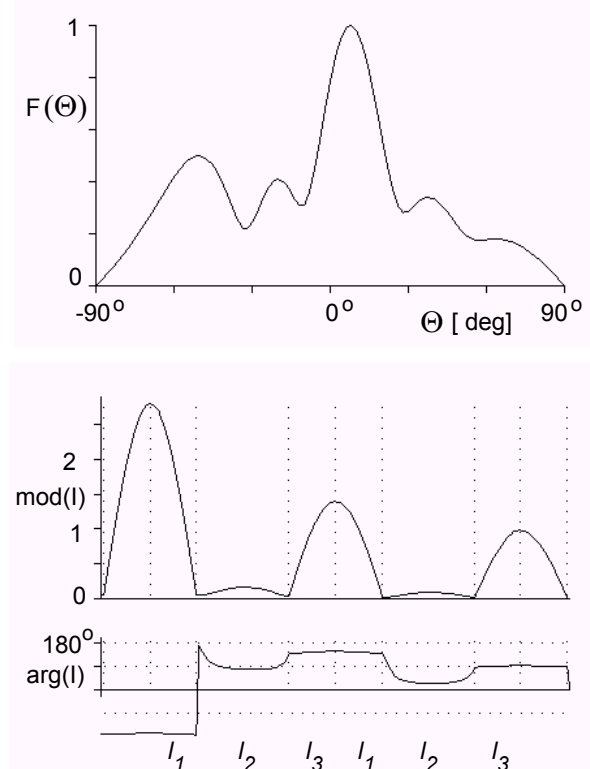


**Fig. 7** Radiation pattern and current distribution of coaxial array.  
 $\alpha l_1 = 90^\circ$ ,  $\alpha l_2 = 180^\circ$ ,  $\alpha l_3 = 90^\circ$ ,  $X_1 = X_2 = -10\ 000 \Omega$ ,  
 $\alpha_g l_k = 390^\circ$ .  $D_{max} = 4.5$ ,  $Z_{in} = (112 - j 43) \Omega$ ,  $\beta \lambda = 0.9$

It is interesting that the main lobe shift depends mainly on the feeder length  $\alpha_g l_k$  and is almost independent on the slot separation  $\alpha(l_1 + l_2 + l_3)$  measured on the outer surface of the feeder (compare Fig. 12).

As the radiation pattern depends only slightly on the outer dimensions of the system, the results in Fig. 7 enable to estimate the usable frequency band of the array. E.g., when the array discussed in Fig. 6 is detuned by 8 % (that means  $\alpha l_1 = \alpha l_3 = 97^\circ$ ,  $\alpha l_2 = 194^\circ$ ), the radiation patterns are practically identical with those in Fig. 7. However, for determination of the frequency band, also the frequency dependence of  $X_1$  and  $X_2$  must be taken into account.

The consequence of finite load of dipole arms ( $X_1, X_2$ ) can be observed in Fig. 8. The antenna grows into an anti-phase array of five half-wave dipoles.

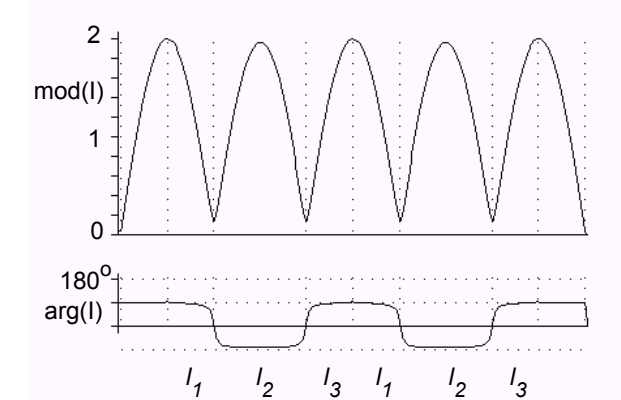
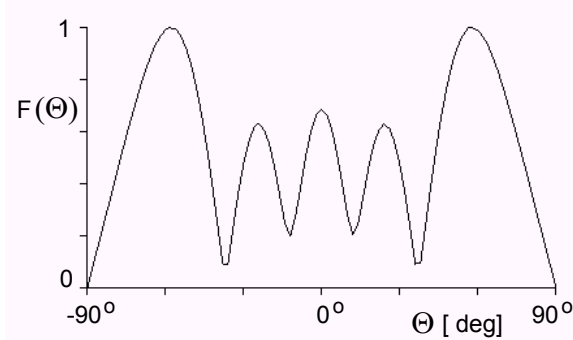


**Fig. 8** Radiation pattern and current distribution of coaxial array.  
 $\alpha l_1 = 90^\circ$ ,  $\alpha l_2 = 180^\circ$ ,  $\alpha l_3 = 90^\circ$ ,  $X_1 = -300 \Omega$ ,  $X_2 = -300 \Omega$ ,  
 $\alpha_g l_k = 360^\circ$ .  $D_{max} = 2.9$ ,  $Z_{in} = (125 - j 40) \Omega$ ,  $\beta \lambda = 0.28^\circ$

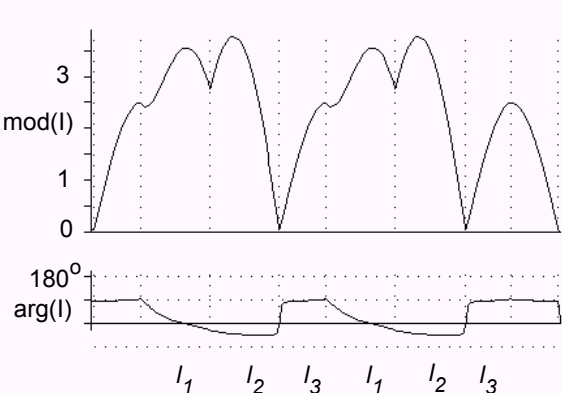
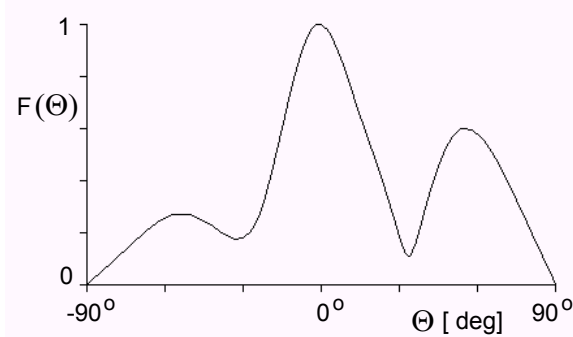


**Fig. 9** Radiation pattern and current distribution of coaxial array.  $\alpha l_1 = 135^\circ$ ,  $\alpha l_2 = 135^\circ$ ,  $\alpha l_3 = 90^\circ$ ,  $X_1 = -300 \Omega$ ,  $X_2 = -10 \text{ k}\Omega$ , and  
 $\alpha_g l_k = 360^\circ$ .  $D_{max} = 3.3$ ,  $\beta \lambda = 0.72$ ,  $Z_{in} = (735 - j 95) \Omega$

Now, we turn our attention to asymmetric dipoles ( $\alpha l_1 \neq \alpha l_3$ ). As far as  $X_1 = X_2 \rightarrow \infty$  and the difference  $|l_2 - l_1|$  does not exceed the value  $\lambda/8$  substantially, the radiation pattern is practically not changed. However, if one arm of each dipole is loaded by a finite reactance, the radiation pattern changes appreciably, the directivity factor drops and the input impedance increases (Fig. 9). When, in addition, the feeder is detuned ( $\alpha_g l_k \neq 360^\circ$ ), the deformation of radiation pattern is significant (Fig. 10). The main lobe direction seems to be shifted by tens of degrees. Unfortunately, this is not right. The "main lobe" (at  $\theta = 47^\circ$ ) is a side lobe and its symmetrically situated counterpart is suppressed due to the coaxial line detuning.

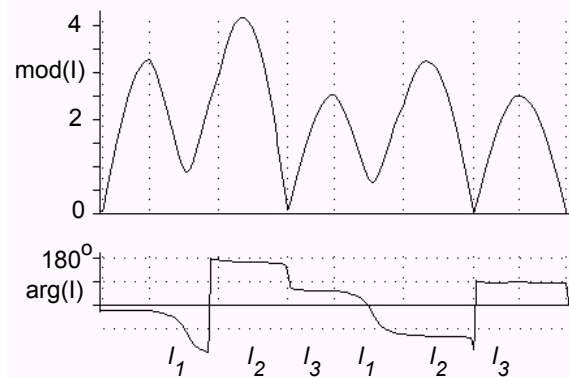
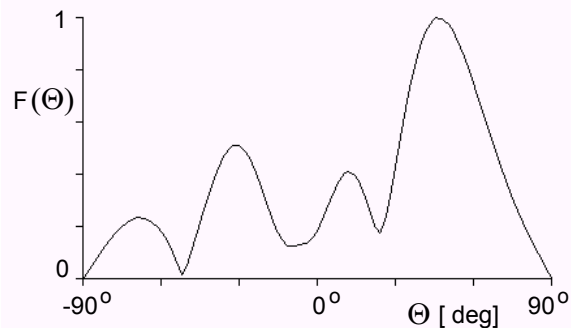


**Fig. 10** Radiation pattern and current distribution of coaxial array.  
 $\alpha l_1 = 135^\circ$ ,  $\alpha l_2 = 135^\circ$ ,  $\alpha l_3 = 90^\circ$ ,  $X_1 = -100 \Omega$ ,  $X_2 = -10 \text{ k}\Omega$ ,  
 $\alpha_g l_k = 330^\circ$ .  $D_{max} = 4.6$ ,  $Z_{in} = (196 + j 24) \Omega$ ,  $\beta \lambda = 0.3$

The following brief set of examples starts from some other idea than the previous one. We suppose that each section alone is an array consisting of 3 identical elements (i.e.  $\alpha l_1 = \alpha l_2 = \alpha l_3$ ). E.g., for  $\alpha l_1 = \alpha l_2 = \alpha l_3 = 120^\circ$ ,  $\alpha_g l_k = 360^\circ$  and  $X_1 = X_2 = -800 \Omega$ , the radiation pattern is nearly identical with that in Fig. 6, but the current distribution as well as the input impedance are quite different. It is interesting that the lengths  $\alpha l_i$  may be shortened and the array keeps still its properties. The array shown in Fig. 11 has the total length of one section only  $0.83 \lambda$  (but  $\alpha_g l_k = 360^\circ$ ) and has a very good sidelobe level (less than 0.2).

In the case presented in Fig. 12, effects of arm shortening and feeder detuning are combined. The main lobe shift about  $20^\circ$  can be reached together with acceptable pattern deformation on a whole.

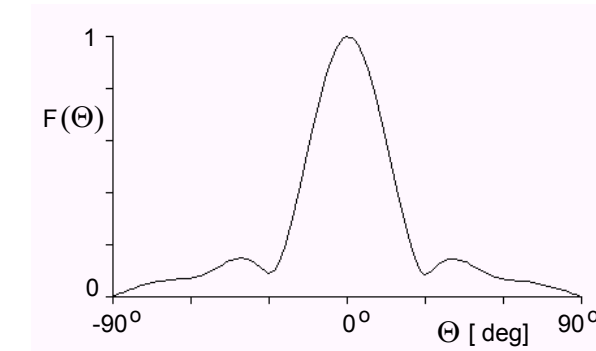


**Fig. 11** Radiation pattern and current distribution of coaxial array.  
 $\alpha l_1 = 100^\circ$ ,  $\alpha l_2 = 100^\circ$ ,  $\alpha l_3 = 100^\circ$ ,  $X_1 = -500 \Omega$ ,  $X_2 = -500 \Omega$ ,  
 $\alpha_g l_k = 360^\circ$ .  $D_{max} = 4.4$ ,  $\beta \lambda = 1.3$ ,  $Z_{in} = (742 + j 267) \Omega$

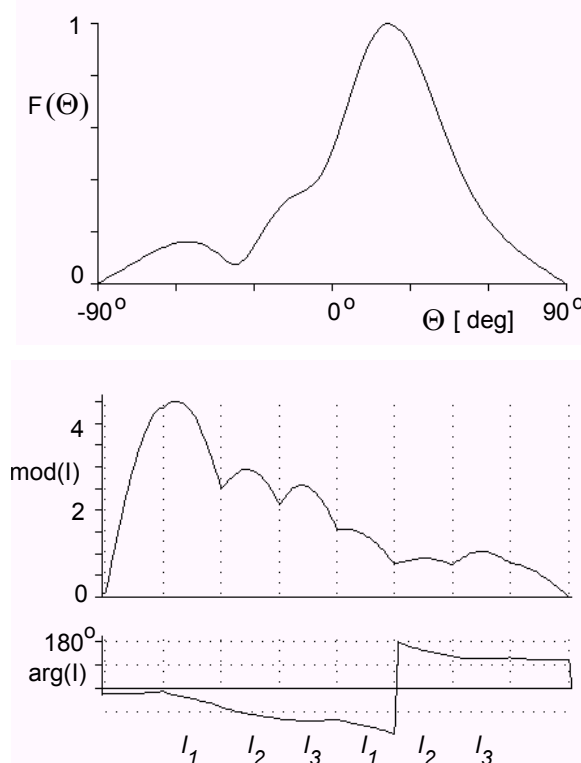


**Fig. 12** Radiation pattern and current distribution of coaxial array.  
 $\alpha l_1 = 90^\circ$ ,  $\alpha l_2 = 90^\circ$ ,  $\alpha l_3 = 90^\circ$ ,  $X_1 = -300 \Omega$ ,  $X_2 = -300 \Omega$ ,  
 $\alpha_g l_k = 390^\circ$ .  $D_{max} = 3.5$ ,  $Z_{in} = (216 - j 43) \Omega$ ,  $\beta \lambda = 1.1$

Till now, we have investigated, how the antenna properties depend on the arrangement and dimensions of its central part. However, properties of the antenna can be apparently affected by the top and bottom parts. From the practical point of view, the bottom part is more important. When the reactance  $X_b$  (see Fig. 5) is not sufficiently great, then the outer surface of the feeder ( $l_{b2}$  in Fig. 5) gets an active part of array and contribute more or less to antenna radiation.

To demonstrate the effect of  $X_b$ , we use the antenna from Fig. 6. Its radiation pattern and other parameters in the ideal case ( $X_b \rightarrow \infty$ ) are known (Fig. 6). When reactance  $X_b$  is reduced to (about)  $300 \Omega$  (e.g., due to the resonator detuning), a small drop of input impedance appears, but the radiation pattern and the directivity factor  $D$  remain practically constant. If the reactance  $X_b$  decreases to  $100 \Omega$  (see Fig. 13), the situation changes drastically. The antenna is (mostly) inapplicable.

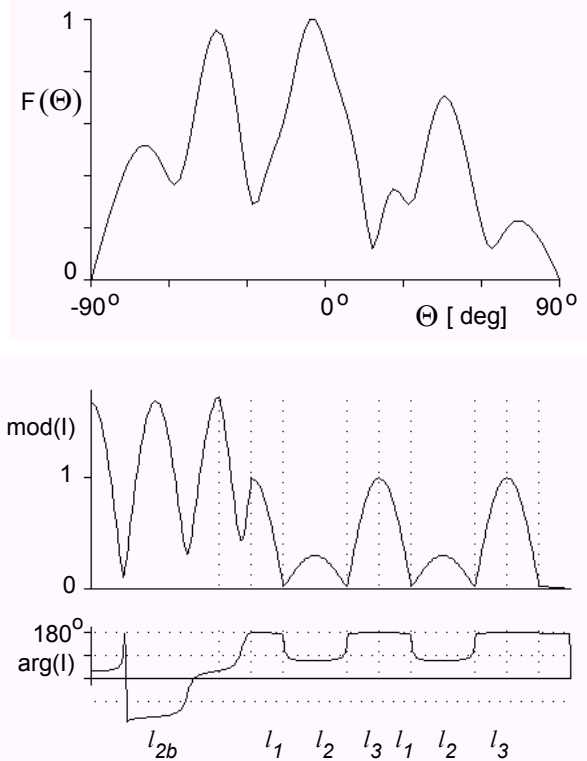


**Fig. 13** Radiation pattern and current distribution of coaxial array.  
 $\alpha l_1 = 180^\circ$ ,  $\alpha l_2 = 90^\circ$ ,  $\alpha l_3 = 90^\circ$ ,  $\alpha l_{2b} = 360^\circ$ ,  $X_1 = -10 \text{ k}\Omega$ ,  
 $X_2 = -10 \text{ k}\Omega$ ,  $X_b = 100 \Omega$ ,  $\alpha_g l_k = 360^\circ$ .  $D_{max} = 4.4$ , and  
 $\beta \lambda = 0.25$ ,  $Z_{in} = (0.8 + j 2.7) \Omega$

A similar effect appears also for the other arrangements of the investigated antenna. But the sensitivity of various arrangements to the magnitude of  $X_b$  is different. For instance, the antenna from Fig. 11 has its radiation pattern similar as the antenna from Fig. 6, but it admits the value  $X_b = 0$  without significant degradation of its properties (Fig. 14).

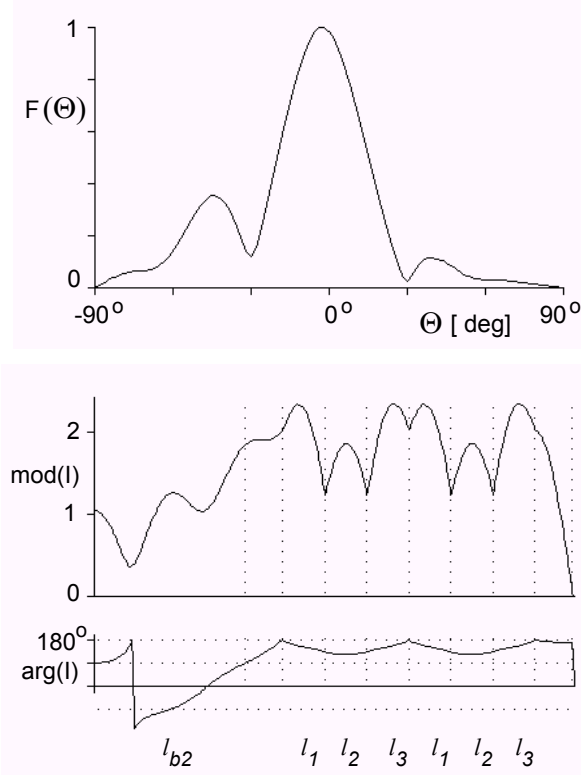


**Fig. 14** Radiation pattern and current distribution of coaxial array.  
 $\alpha l_1 = 100^\circ$ ,  $\alpha l_2 = 100^\circ$ ,  $\alpha l_3 = 100^\circ$ ,  $\alpha l_{b2} = 360^\circ$ ,  $X_1 = -500 \Omega$ ,  
 $X_2 = -500 \Omega$ ,  $X_{b1} = 0 \Omega$ ,  $\alpha_g l_k = 360^\circ$ ,  $D_{max} = 4.4$ ,  $\beta \lambda = 1.1$ ,  
 $Z_{in} = (742 + j 267) \Omega$

## 6. Conclusion

As the previous examples demonstrate, the slot-fed coaxial dipole array presents radiation pattern of different kind: pattern with normal (horizontal) radiation, with elevated radiation or with multilobe radiation (antiphase array). The input impedance (of two-section array) is mostly several hundreds ohms and the absolute gain (related to the isotropic source) is about 5 - 7 dB. The usable frequency band depends on individual requirements but the antenna operates typically as narrow band antenna ( $\Delta f < 0.01 f_0$ ). Several optional parameters enable to match the antenna properties to various requirements.

## Acknowledgement

The project has been supported the research plan No. MSM 262200011 *Research of Electronic and Communication Systems and Technologies*.

## References

- [1] ČERNOHORSKÝ, D., NOVÁČEK, Z. Radiation pattern and impedance of dipole excited by a slot in its coaxial feeder. In Proceedings of the International Conference Radioelektronika 2001. Brno: Brno University of Technology, 2001, vol. 1, p. 250 – 253.
- [2] HAUŠKA, M. Klasický antifading či ARPO? (A classical anti-fading or ARPO?). Telekomunikace. 1979, vol. 5, no. 6, p. 83–86.
- [3] AJZENBERG, G. Z. Kurzwellenantennen (Short-wave antennas). Leipzig: Fachbuchverlag, 1954.

## About authors...

**Dušan ČERNOHORSKÝ** was born in 1930 in Prague, Czech Republic. He received the Ing. (M.Sc.) degree in 1954 and the CSc. (Ph.D) degree in 1965, both from the Military Technical Academy, Brno, Czech Republic. In 1964, he spent one year at the Military Engineering College in Cairo (Egypt). Since 1970, he worked as Associated Professor, and since 1991 as Professor with the Institute of Radio Electronics at the Brno University of Technology. His interests include EM field theory and antenna theory and practice. His main research domains are short wave and mobile antennas, adaptive antennas and the space-time signal processing.

**Zdeněk NOVÁČEK** was born in 1945 in Kamenná, Czech Republic. He received the Ing. (M.Sc.) degree in 1969 and the CSc. (Ph.D) degree in 1980, both from the Brno University of Technology. Since 1969, he worked as Senior lecturer and since 1997 as Associate Professor at the Institute of Radio Electronics at the BUT Brno. He is interested in EM field , antennas and propagation of radio waves. His research includes mobile antennas, antenna measurements and the space-time signal processing.